

## NUMERICAL METHOD FOR CALCULATING SURFACE CURRENT DENSITY ON A TWO-DIMENSIONAL SCATTERER WITH SMOOTH CONTOUR

K. Yasuura

Department of Computer Science and Communication Engineering,  
Kyushu University, Fukuoka 812, Japan

Y. Okuno

Department of Electronic Engineering, Kumamoto University, Kumamoto 860, Japan

### 1. INTRODUCTION

Numerical methods for the two-dimensional scattering problems can be classified broadly into two categories: integral equation approach and modal expansion approach. When we employ the former, we usually formulate an integral equation with respect to the surface current density. We then solve the equation numerically with a careful consideration not to yield a resonance solution and compute the scattered field by an integral over the cross section of the scatterer. On the other hand, in the latter approach we find an approximation of the scattered field directly by fitting a truncated modal expansion to the boundary condition of the problem.

The mode-matching method with a smoothing procedure (MMM with SP)[1-3] which we presented as a powerful numerical technique for the problems with smooth boundaries belongs to the latter: we can obtain the scattered field without calculating the current density. However, we cannot neglect the current density since it is an important physical quantity itself and is sometimes required for engineering application.

In the following sections we state an approximation method for the current density. The method is closely related to the MMM with the SP: the method leads us to solve a set of linear equations being adjoint to one which, when we employ the MMM with the SP, determines the coefficients of the scattered field. That is, there holds a duality between scattered field approximation by the MMM with the SP and current density approximation by the method of this paper. The time factor  $\exp(i\omega t)$  will be suppressed throughout.

### 2. FORMULATION OF THE PROBLEM

We consider a cylindrical scatterer made of a perfect electric conductor. Figure 1 shows the cross section of the scatterer and coordinate system. We assume that the contour  $C$  is sufficiently smooth and that it has a unit length. When an E-polarized plane wave

$$\mathbf{E}^i(\mathbf{P}) = \mathbf{a}_z F(\mathbf{P}), \quad F(\mathbf{P}) = \exp[-ik\rho_p \cos(\theta_p - \theta_1)] \quad (1)$$

hits the cylinder, a surface current flows along the  $z$  direction to induce a scattered field  $\Psi(\mathbf{P})$  and hence the total electric field outside  $C$  becomes

$$\Phi(\mathbf{P}) = F(\mathbf{P}) + \Psi(\mathbf{P}). \quad (2)$$

The surface current density  $K(s)$ , which we seek, is given by

$$K(s) = -(i\omega\mu)^{-1} \partial\Phi(s)/\partial\nu \quad (3)$$

where  $\nu$  is the coordinate along the inward normal to the contour  $C$ .

### 3. METHOD OF NUMERICAL ANALYSIS

We state the method being adjoint to the MMM with the SP. First we put

$$j(s) = -i\omega\mu K(s) = \partial\Phi(s)/\partial\nu, \quad (4)$$

and we describe the approximation method for the  $j(s)$  for simplicity.

We introduce the modal functions by

$$\phi_m(P) = H_m^{(2)}(k\rho_p) \exp(-im\theta_p) \quad (5)$$

$m = 0, \pm 1, \pm 2, \dots$

where  $H_m^{(2)}$  stands for the  $m$  order second type Hankel function. Note that they are radiative solutions of the two-dimensional Helmholtz equation obtained by separation of variables.

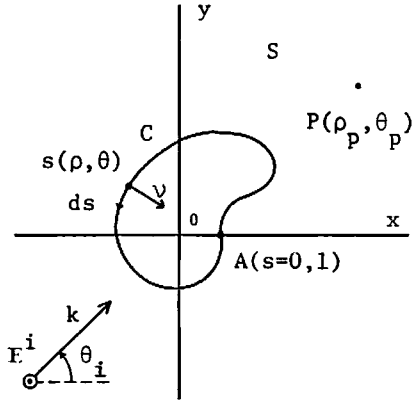


Fig. 1 Geometry of the problem.

Since the contour of the scatterer is sufficiently smooth, the derivative

$$f(s) = dj(s)/ds \quad (6)$$

is continuous and is orthogonal to constants,  $(1, f) = 0$ .<sup>+</sup>

We define an approximate derivative  $f_N(s)$  by

$$f_N(s) = \sum_{m=-N}^N C_m(N) \mathbb{K} \phi_m^*(s). \quad (7)$$

Here,  $\phi_m^*$  denotes the complex conjugate of  $\phi_m[\phi_m^*(s) = H_m^{(1)}(k\rho) \exp(im\theta)]$  and  $\mathbb{K}$  is an integral operator defined by

$$\mathbb{K}\psi(s) = \int_0^1 K(s, t) \psi(t) dt, \quad K(s, t) + (s-t) = -1/2 \quad (s < t); = 1/2 \quad (s > t) \quad (8)$$

Note that  $\mathbb{K}\psi(s)$  is an indefinite integral of  $\psi_{\perp}(s) [= \psi(s) - (1, \psi)]$  and is orthogonal to constants.

We decide the  $C_m$  coefficients so that  $f_N(s)$  becomes the best approximation of  $f(s)$  in the mean squares sense, i.e.,

$$\| \| f_N - f \| \| \rightarrow \text{minimum}^{++} \quad (9)$$

under the constraint that

$$(1, \sum_{m=-N}^N C_m(N) \phi_m^*) = 0. \quad (10)$$

We can prove that the sequence of the approximate derivatives  $\{f_N(s): N=0, 1, 2, \dots\}$  with the coefficients determined by the above manner converges to the true derivative in the mean squares sense. The proof is similar to that of the convergence theorems stated in Refs. 1 and 2. Practically, the coefficients satisfying (9) and (10) are obtained by the following set of equations:

$$\sum_{m=-N}^N C_m(N) ((\phi_m, \phi_n)) + (1, \phi_n) v_N = \langle F, \phi_n \rangle \quad |n| \leq N$$

$$\sum_{m=-N}^N C_m(N) (\phi_m, 1) = 0 \quad (11)$$

Here, the double parentheses mean the inner product defined by

$$((\phi, \psi)) = (\mathbb{K}\phi, \mathbb{K}\psi) \quad (12)$$

<sup>+</sup> The inner product is defined by  $(\phi, \psi) = \int_0^1 \phi^*(s)\psi(s) ds$ .

<sup>++</sup> The norm is understood in the mean squares sense:  $\| \psi \| = (\psi, \psi)^{1/2}$ .

which can be evaluated by a weighted double integral with a weighting kernel  $K^2(s,t)$ , the second order recurrent kernel of  $K(s,t)$ . [1,2] The  $v_N$  coefficient is defined by

$$v_N = \mu_N - (1,j) \quad (13)$$

with  $\mu_N$  being the Lagrange multiplier corresponding to the constraint (10). The notation  $\langle F, \phi_n \rangle$  which also appeared in (11) stands for the reaction [4,5] between  $F(P)$  and  $\phi_n(P)$  and is given by

$$\langle F, \phi_n \rangle = -4i \exp[-in(\theta_1 + \pi/2)]. \quad (14)$$

We make an approximation for the  $j(s)$  by putting

$$j_N(s) = \mathbb{K}f_N(s) - v_N = \sum_{m=-N}^N C_m(N) \mathbb{K}^2 \phi_m^*(s) - v_N \quad (15)$$

where  $\mathbb{K}^2$  means an iterative operation of  $\mathbb{K}$ :  $\mathbb{K}^2\psi(s) = \mathbb{K}(\mathbb{K}\psi)(s)$ . We can prove the fact that the sequence  $\{j_N(s): N=0, 1, 2, \dots\}$  converges to  $j(s)$  uniformly on the contour  $C$ , i.e.,  $0 \leq s \leq 1$ .

Next we show that a duality holds between the current density approximation by the above method and the scattered field approximation by the MMM with the SP. [1-3] We make an approximate scattered field by

$$\Psi_N(P) = \sum_{n=-N}^N A_n(N) \phi_n(P). \quad (16)$$

The unknown coefficients are chosen so that the quantity  $\|\mathbb{K}(\Psi_N + F)\|$  becomes to be minimum under the constraint that  $(1, \Psi_N + F) = 0$ . This leads us to solve a set of linear equations which is strictly adjoint to (11) except that the force terms become  $-(\phi_m, F)$  ( $|m| \leq N$ ).

Although we concentrated our discussion on the numerical method which is adjoint to the MMM with the first order SP, we can establish the algorithms which are adjoint to the conventional MMM [5] or the MMM with a higher-order SP. [2] In the next section we employ all of them [the  $p=0$  method (adjoint to the conventional MMM), the  $p=1$  method (adjoint to the MMM with the first order SP, the method in this section) and the  $p=2$  method (adjoint to the MMM with the second order SP)] for a sample calculation and compare the results.

#### 4. NUMERICAL EXAMPLES AND DISCUSSION

We calculate the approximations for the  $j(s)$  by the three methods on a surface of a scatterer whose cross section is composed of a semi-circle with the radius  $b$  and a semi-ellipse with the semi-majoraxis  $a$ . The following results are obtained under the conditions that  $a/b=1.5$ ,  $kb=2.5899$  and  $\theta_1=90^\circ$ . The shape of the scatterer is shown in Fig. 2.

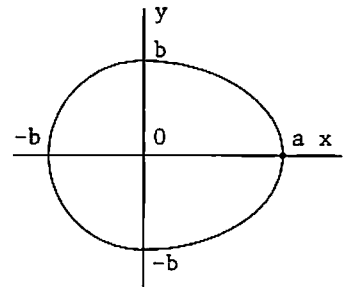


Fig. 2 The scatterer for sample calculation.

In Fig. 3 we compare the rates of convergence of the solutions obtained by the three methods. Note that the sequence of solutions  $\{j_N^1(0): N=8, 10, \dots\}$  approaches to  $j_\infty^0(0)=15.67/54.7^\circ$  more rapidly than the sequence  $\{j_N^0(0): N=8, 10, \dots\}$ . Also the Sequence  $\{j_N^2(0): N=8, 10, \dots\}$  converges faster than  $\{j_N^1(0): N=8, 10, \dots\}$ .

Next we examine the three methods from the viewpoint of the extended boundary condition: the secondary field  $\Psi(P)$  induced by the surface current must cancel the incident field inside the scatterer. We define the error on the extended boundary condition by

$$EEBC(p, N) = \max_{P \in D} |F(P) + \Psi_N^P(P)| / |F(P)| \quad (17)$$

where  $D$  is a subdomain inside the contour  $C$  and the boundary of  $D$  is similar to  $C$  with a ratio of similitude 0.9. In (17),  $\Psi_N^P(P)$  should be calculated from the approximate current density through the usual integral representation using the free space Green function. The resultant errors are  $EEBC(0,10)=3.3\%$ ,  $EEBC(1,10)=1.5\%$  and  $EEBC(2,10)=0.8\%$ .

We show in Fig. 4 the entire view of the approximate current density obtained by the  $p=0$  (the dots) and the  $p=2$  (the solid curves) methods with the number of truncation 10. We find in this figure that the  $p=2$  solution has almost converged while the  $p=0$  solution behaves oddly and has not converged yet.

It becomes clear from the above discussions that the method with the smoothing procedure (the  $p=1$  and the  $p=2$  methods) are effective numerical algorithms for finding the surface current density.

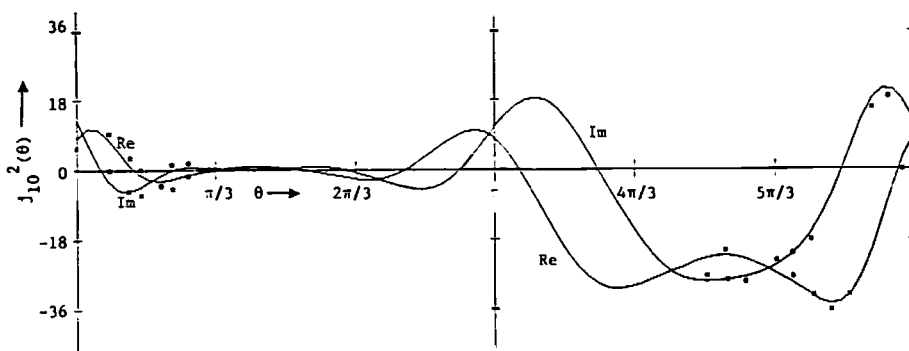


Fig. 4 Current densities obtained by the  $p=2$  (solid curve) and the  $p=0$  (dots) methods.

REFERENCES: [1] H. Ikuno and K. Yasuura, *Radio Sci.*, 13, 937-946(1978), [2] Y. Okuno and T. Matsuda, *J. Opt. Soc. Am.*, 73, 1305-1311(1983), [3] K. Yasuura and Y. Okuno, *J. Opt. Soc. Am.*, 72, 847-852(1982), [4] V. H. Rumsey, *Phys. Rev.*, 94, 1483-1491(1954), [5] K. Yasuura, *Progress in Radio Science 1966-1969*, URSI-Brussels, 257-270(1971).

ACKNOWLEDGEMENTS: The authors wish to express their thanks to Professor T. Itakura of Kumamoto University for useful discussions. Also we thank Mr. K. Murakawa of Kumamoto University for his contribution to numerical computations.

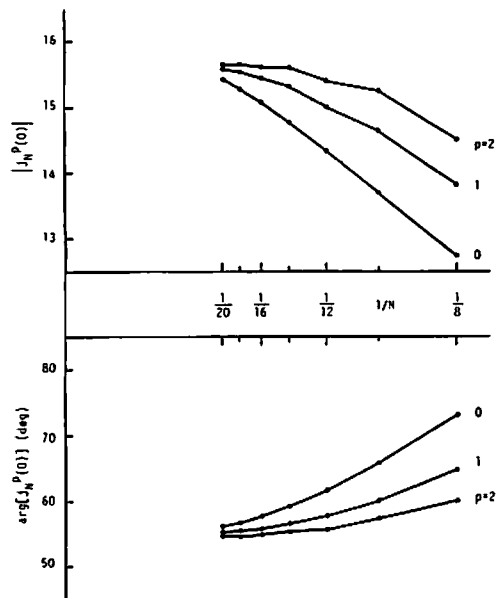


Fig. 3 Comparison of the convergence rates of  $j_N^P(0)$  ( $p=0, 1$  and  $2$ ).